The Sub-Parabolic Lines of a Surface

Richard Morris,
Department of Applied Mathematics and Theoretical Physics,
University of Liverpool,
PO Box 147, Liverpool, L69 3BX,
email rmorris@liv.ac.uk

July 10, 1997

Introduction

In this paper we will study various significant curves on surfaces, in particular the ridges and sub-parabolic lines. Whereas the parabolic lines capture the second derivative information about a surface, the ridges and sub-parabolic lines capture the third derivative information about the surface.

One important feature of the ridges and sub-parabolic lines is that, like the parabolic curves, they are *robust*, i.e. if we slightly deform the surface then the curve will *deform*. This contrasts with the geodesics and lines of curvature of the surface which *reform* as the surface is deformed. Hence it makes sense to observe how a sub-parabolic line changes in a family of surfaces but it does not make sense to study how a line of curvature changes.

The ridges can be thought of as the set of points where one of the principal curvatures has an extremal value (max or min), when moving along a line of curvature of the same colour. They can also be thought of as the pre-image of cuspidal edges on the focal surface. I. Porteous first gave the curves a thorough mathematical treatment in [12], which was expanded on in [13], by studying the singularities of the distance squared map. An alternative approach used in [4], [21] and [2] is to consider folding maps of the surface, which captures the local reflectional symmetry. Two papers on ridges have previously been presented in this series of conferences, [14] [15].

In [8], J. Koenderink recognised that ridges are significant features of a surface and they are beginning to find several applications. They have been used by Thirion and Gourdon in the study of medical Magnetic Resonance Image data [20]. G. Gordon, D. Mumford has used them for face recognition from range data [7]. In geology the ridges appear as the hinge lines of folds, [18].

Whilst not being as visually obvious as ridges, the significance of sub-parabolic lines is increasing. They were first observed as the pre images of parabolic lines on the focal surface, hence the name. They also appear as the *locus of geodesic inflections*, of the lines of curvature. For this reason Porteous has proposed the shorter name *flexcords* for these curves. We shall see later that the a recent result of Thirion suggests an alternative characterisation: as the *counter-ridges*, points where the principal curvature of one colour has an extremal value when moving along a line of curvature of the other colour. Sub-parabolic lines can be found by examining the profiles of surfaces. Sub-parabolic lines have a fairly short history, first being studied in terms of folding maps in [4] and [21]. In [11] they are studied geometrically in terms of the focal surface and the distance

squared function and experimentally where examples of the transitions were found by computer. In [2] and [3] the transitions which occur on both curves are discussed.

One early reference is Eisenhart [6] where an explicit equation for the Gaussian Curvature of the focal surface is presented. In his recent book [16] Porteous gives both ridges and sub-parabolic lines a thorough treatment.

In section §1 we present some basic facts about surfaces and focal surfaces. In section §2 we present simple proofs for the characterisations of sub-parabolic lines and ridges and also discuss the Gaussian curvature of the focal surface. Section §3 deals with the special points which can occur on these curves, including the highly spherical umbilic points. Some practical formulae for calculating the curves for implicit and explicitly defined surfaces are discussed in section §4 as well as some of the problems which may occur in a computer implementation. Finally, in section §5 we discuss some of the possible applications of these curves.

Many thanks to Ian Porteous for help in the preparation of this paper.

1 Basic Geometry of Surfaces

At a generic point on a smooth surface S we can find two *principal directions* $\underline{P}$, $\underline{Q}$, and two corresponding *principal curvatures* κ_p, κ_q such that the normal curvature of a curve through x with tangent to $\underline{P}$ or $\underline{Q}$ is κ_p or κ_q respectively. Furthermore, κ_p and κ_q are the extremal values of the normal curvatures for all smooth curves through x. (The normal curvature of a curve on S with tangent $\underline{V}$ is the curvature of the intersection of the surface and the plane containing the normal and $\underline{V}$.) We can give these principal directions a colour (red or blue) to distinguish between the two. In the following let $\underline{P}$ be the *red* principal direction and $\underline{Q}$ be the *blue* principal direction. We make no assumption about which corresponds to the higher or lower principal curvature but the colours are assigned consistently. It is well known that the normal to the surface, $\underline{N}$, and the two principal directions are all orthogonal.

We also expect to find isolated points on the surface where the surface closely approximates a sphere. At these points, called *umbilics*, every direction through the umbilic is principal and all the principal curvatures are equal.

We can also consider the focal surface. This consist of two sheets, the red and blue sheet. For any point on the surface there are two points on the focal surface f_p, f_q given by $x + 1/\kappa_p \underline{N}$ and $x + 1/\kappa_q \underline{N}$. The focal surface can be considered as the envelope of the normals to the surface. Figure 1 shows the geometry of the surface and its focal surfaces.

A line of curvature is a curve whose tangent is always in a principal direction. Again there are two sets of lines of curvature, red and blue, according to which principal direction they are tangent to. The normal curvature of these curves is always the principal curvature, but we can also find the *geodesic curvature* of these curves which is the curvature of the curve when projected on to the tangent plane. We can also think about the *raised lines of curvature*. If we take a line of curvature on a surface, then there is a corresponding line on each sheet of the focal surface. These lines are called the raised lines of curvature and it can be shown that a red line of curvature raised to the red sheet of the focal surface is a geodesic.

1.1 Directional Derivatives

The notation will be greatly simplified if we use directional derivatives. If $f : \mathbf{R}^2 \to \mathbf{R}^n$ and $u = (u_1, u_2)$ is a tangent vector to $\mathbf{R}^2$, then the *directional*

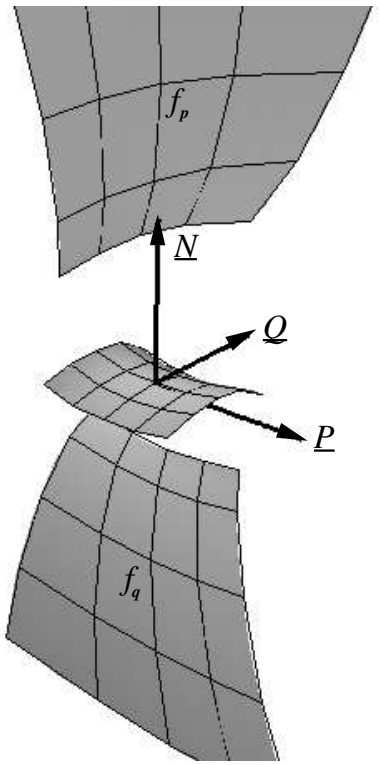

Figure 1: The basic geometry of a surface and its focal surfaces

derivative of f in the u direction is

$$df<\underline{u}> = u_1 \frac{\partial f}{\partial x} + u_2 \frac{\partial f}{\partial x}.$$

We can see that df is a linear map which is indicated by the angled brackets. This notation can be extended to higher dimensions and also to higher derivatives. The second directional derivatives of f in directions $u = (u_1, u_2)$, $v = (v_1, v_2)$ is

$$d^2 f<uv> = u_1 v_1 \frac{\partial^2 f}{\partial x^2} + (u_1 v_2 + u_2 v_1) \frac{\partial^2 f}{\partial x \partial y} + u_2 v_2 \frac{\partial^2 f}{\partial^2 y}.$$

We observe that this map is a symmetric bilinear form.

1.2 The First and Second Fundamental Forms of a Surface

For a surface S parametrised by $s : \mathbf{R}^2 \to \mathbf{R}^3$, with normal $\underline{N}$. We can define two symmetric bilinear forms

$$\begin{aligned} I_s<u, v> &= ds<u> \cdot ds<v>, \\ II_s<u, v> &= ds<u> \cdot d\underline{N}<v> \\ &= -d^2 s<uv> \cdot n, \end{aligned}$$

called the *first* and *second fundamental forms of the surface* S. The eigen-vectors of the equation $II_s<u, v> = \kappa I_s<u, v>$ give the principal directions p, q. These vectors lie in the parameter space, and we can choose them so that $\underline{P} = ds<p>$,

and $\underline{Q} = ds<q>$ are unit length vectors. We have the following results

$$\begin{aligned}
I_s<pp> &= 1,\\
I_s<pq> &= 0,\\
I_s<qq> &= 1,\\
II_s<pp> &= -d\underline{N}<p> \cdot \underline{P} = \kappa_p,\\
II_s<pq> &= -d\underline{N}<q> \cdot \underline{P} = -d\underline{N}<p> \cdot \underline{Q} = 0,\\
II_s<qq> &= -d\underline{N}<q> \cdot \underline{Q} = \kappa_q.
\end{aligned}$$

As $\underline{N} \cdot \underline{P} = 0$ and $\underline{N} \cdot \underline{Q} = 0$ we can deduce

$$\begin{aligned}
d\underline{P}<p> \cdot \underline{N} = \kappa_p,\\
d\underline{P}<q> \cdot \underline{N} = 0,\\
d\underline{Q}<p> \cdot \underline{N} = 0,\\
d\underline{Q}<q> \cdot \underline{N} = \kappa_q.
\end{aligned}$$

2 The geometry of ridges and sub-parabolic lines

In this section we give precise definitions for the ridges and sub-parabolic lines, and also show that the three characterisations are equivalent. We begin with a simple lemma about the focal surface.

Lemma 1 *The tangents to the images of the lines of curvature on the red (p) sheet of the focal surface are*

$$\begin{aligned}
df_p<p> &= -d\kappa_p<p>/\kappa_p^2 \underline{N},\\
df_p<q> &= -d\kappa_p<q>/\kappa_p^2 \underline{N} + (\kappa_p - \kappa_q)/\kappa_p \underline{Q}.
\end{aligned}$$

In particular, $\underline{P}$ is normal to the focal surface.

Proof
Now

$$\begin{aligned}
(f_p(x) - s(x)) \cdot \underline{P} &= 0,\\
(f_p(x) - s(x)) \cdot \underline{Q} &= 0,\\
(f_p(x) - s(x)) \cdot \underline{N} &= 1/\kappa_p.
\end{aligned}$$

Differentiating in the r direction gives

$$\begin{aligned}
(df_p<r> - ds<r>) \cdot \underline{P} + 1/\kappa_p \underline{N} \cdot d\underline{P}<r> &= 0,\\
(df_p<r> - ds<r>) \cdot \underline{Q} + 1/\kappa_p \underline{N} \cdot d\underline{Q}<r> &= 0,\\
(df_p<r> - ds<r>) \cdot \underline{N} + 1/\kappa_p \underline{N} \cdot d\underline{N}<r> &= -d\kappa<r>/\kappa_p^2.
\end{aligned}$$

Substituting $r = p$ and $r = q$ gives

$$\begin{aligned}
df_p<p> \cdot \underline{P} &= 0,\\
df_p<q> \cdot \underline{P} &= 0,\\
df_p<p> \cdot \underline{Q} &= 0,\\
df_p<q> \cdot \underline{Q} &= 1 - \kappa_q/\kappa_p,\\
df_p<p> \cdot \underline{N} &= -d\kappa<p>/\kappa_p^2,\\
df_p<q> \cdot \underline{N} &= -d\kappa<q>/\kappa_p^2.
\end{aligned}$$

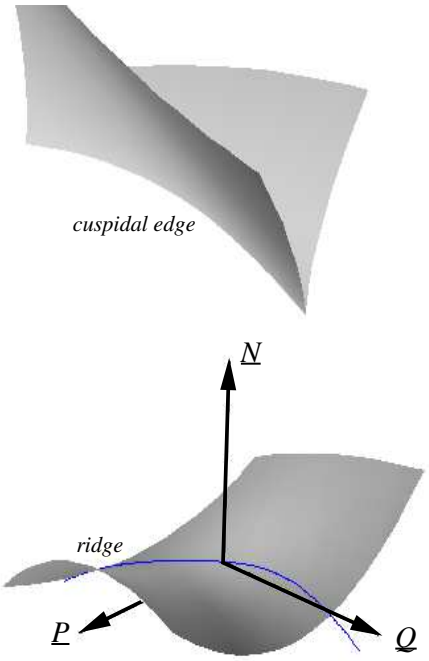

Figure 2: The geometry of the surface and focal surface about a ridge point.

□

We can now make the definition of ridges and sub-parabolic lines more precise.

Definition 2 *A point x lies on a* red-ridge *when $d\kappa_p<p>$ is zero. A point x lies on a* red-subparabolic *line when $d\kappa_q<p>$ is zero.*

We can see from Lemma 1 that the condition for ridges, $df_p<p> = 0$, implies that the focal surface is singular at ridge points, it can be shown that in general we have a cuspidal edge on the focal surface (Fig. 2). For sub-parabolic lines we have the following result, part 3 of which was first proved by Thirion.

Theorem 3 *Away from ridges, parabolic lines and umbilics, the following statements are equivalent.*

1. *The red-sheet of the focal surface has a parabolic line at $f_p(x)$.*
2. *The geodesic curvature of the blue-line of curvature is zero at x.*
3. *$d\kappa_q<p> = 0$ at x.*

Each of these being equivalent to x lying on a red sub-parabolic line.

Proof
We will show that all three statements are equivalent to $d\underline{P}<q> \cdot \underline{Q} = 0$.

Now $\underline{P}$ is normal to the red sheet of the focal surface so for a parabolic line we require $d\underline{P}<r> = 0$ for some vector r. Now $d\underline{P}<r> \cdot \underline{N} = -\underline{P} \cdot d\underline{N}<r> = II<pr>$ which is zero only when $r = q$ or when κ_p is zero, which is non generic.

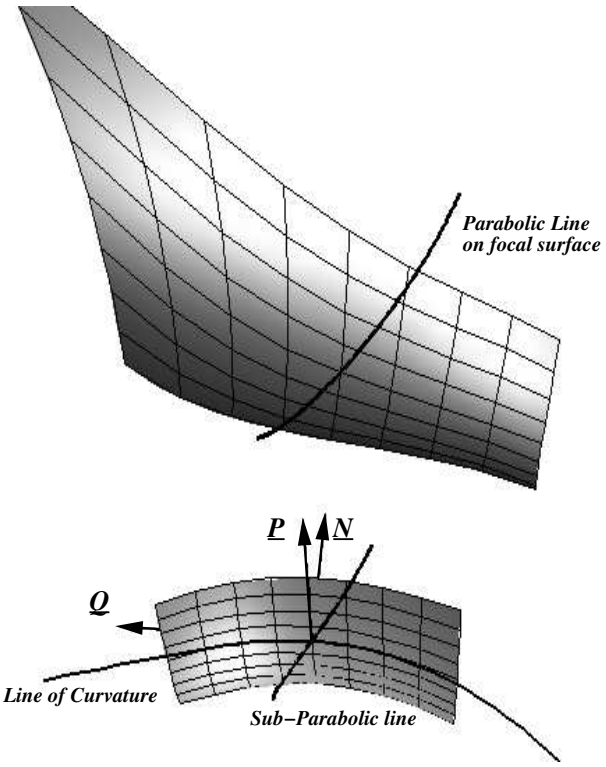

Figure 3: The geometry of the surface and focal surface about a sub-parabolic line.

As $\underline{P}$ is of unit length we see condition for a parabolic line on the focal surface is $d\underline{P}<q> \cdot \underline{Q} = 0$.

Differentiating $\underline{P} \cdot \underline{Q} = 0$ shows that $d\underline{Q}<q> \cdot \underline{P} = -d\underline{P}<q> \cdot \underline{Q}$. Now, $d\underline{Q}<q> \cdot \underline{P} = 0$ is the condition for the blue line of curvature to have an inflection, which proves part 2 of the theorem.

For the final part we observe that on the *blue* sheet of the focal surface

$$\begin{aligned} df_q<p> \cdot d\underline{Q}<q> &= II_{f_q}<pq> \\ &= df_q<q> \cdot d\underline{Q}<p> \\ &= \alpha \underline{N} \cdot d\underline{Q}<p> \\ &= \alpha II<pq> \\ &= 0, \end{aligned}$$

where II_{f_q} is the second fundamental form of the blue sheet of the focal surface. Resolving this equation into the $\underline{N}$ and $\underline{Q}$ components gives

$$(df_q<p> \cdot \underline{N})(d\underline{Q}<q> \cdot \underline{N}) + (df_q<p> \cdot \underline{P})(d\underline{Q}<q> \cdot \underline{P}) = 0.$$

Generically neither $d\underline{Q}<q> \cdot \underline{N}$ nor $df_q<p> \cdot \underline{P}$ is zero so we see $d\underline{Q} \cdot \underline{P} = 0$ is equivalent to $df_q<p> \cdot \underline{N} = 0$. From Lemma 1 we see this implies $d\kappa_q<p> = 0$. □

The generic geometry of the surface and the focal surface for a sub-parabolic line is illustrated in figure 3. Note how we have a parabolic line on the focal surface and that the line of curvature has an inflection. We can gain further information about the surface by considering the Gaussian Curvature of the focal surface.

Theorem 4 *The Gaussian curvature of the focal surface is*

$$K_f = \frac{d\underline{P}<q> \cdot \underline{Q}}{d\kappa_p<p>} \frac{\kappa_p^4}{(\kappa_p - \kappa_q)}.$$

Proof
The Gaussian curvature can be found by calculating $(ln - m^2)/(EG - F^2)$ where

$$\begin{aligned} E &= df_p<p> \cdot df_p<p>, \\ F &= df_p<p> \cdot df_p<q>, \\ G &= df_p<q> \cdot df_p<q>, \\ l &= d\underline{P}<p> \cdot df_p<p>, \\ m &= d\underline{P}<q> \cdot df_p<p>, \\ n &= d\underline{P}<q> \cdot df_p<q>. \end{aligned}$$

Now

$$\begin{aligned} df_p<p> &= \frac{-d\kappa_p<p>}{\kappa_p^2} \underline{N}, \\ df_p<q> &= \frac{-d\kappa_p<q>}{\kappa_p^2} \underline{N} + \left(1 - \frac{\kappa_q}{\kappa_p}\right) \underline{Q}, \\ d\underline{P}<p> &= (d\underline{P}<p> \cdot \underline{Q})\underline{Q} + \kappa_p \underline{N}, \\ d\underline{P}<q> &= (d\underline{P}<q> \cdot \underline{Q})\underline{Q}. \end{aligned}$$

Hence

$$\begin{aligned} E &= (d\kappa_p<p>)^2/\kappa_p^4, \\ F &= d\kappa_p<p> d\kappa_p<q>/\kappa_p^4, \\ G &= (d\kappa_p<q>)^2/\kappa_p^4 + (\kappa_p - \kappa_q)^2/\kappa_p^2, \\ l &= -d\kappa_p<p>/\kappa_p, \\ m &= 0, \\ n &= (d\underline{P}<q> \cdot \underline{Q})(\kappa_p - \kappa_q)/\kappa_p. \end{aligned}$$

Substituting these values into the equation for Gaussian curvature proves the result. □

There are several points to note from this equation.

Corollary 5 *The Gaussian curvature generically changes sign through zero when we cross a parabolic line on the focal surface.*

Corollary 6 *The Gaussian curvature generically changes sign through infinity when we cross a cuspidal edge on the focal surface.*

This second corollary runs counter to what happens in the standard model of a cuspidal edge, (x^2, x^3, y), where the Gaussian curvature is everywhere zero (Fig. 4a). For symmetrical cuspidal edges, like $(x^2 + y^2, x^3, y)$, the curvature is the same sign on either side of the edge (Fig. 4b). In terms of the Gaussian curvature the edge $(x^2, x^3 + y^2, y)$ is more generic, as the curvature changes sign, through infinity, as we cross the edge. We can attach three numbers to a cuspidal edge to describe the way it curves. Let $\gamma(t)$ be a parameterisation of a ridge, with tangent $r = \gamma'(t)$, such that $df_p<r>$ is of unit length. Let

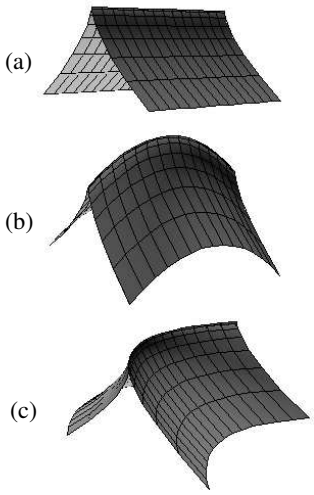

Figure 4: The standard model of a cuspidal edge (a), a symmetric cuspidal edge (b), and a more generic cuspidal edge (c)

$\underline{A} = df_p<r>$, $\underline{B} = \underline{P}$, and $C = \underline{B} \wedge \underline{A}$. We can write the derivatives of these vectors with respect to t as

$$\begin{pmatrix} \underline{A}' \\ \underline{B}' \\ \underline{C}' \end{pmatrix} = \begin{pmatrix} 0 & \kappa & g \\ -\kappa & 0 & \tau \\ -g & -\tau & 0 \end{pmatrix} \begin{pmatrix} \underline{A} \\ \underline{B} \\ \underline{C} \end{pmatrix}.$$

The three numbers κ, g, τ describe the way in which the cuspidal edge curves; κ corresponds to the normal curvature of a curve on a surface, g corresponds to the geodesic curvature and τ corresponds to the "geodesic torsion". See section §1 and also [8] p197.

Lemma 7 *For a generic point on a cuspidal edge of a focal surface, the normal curvature of the edge, κ, is non-zero. Furthermore, away from swallowtail and umbilic centres, κ is zero if and only if $d\underline{P}<q> \cdot \underline{Q}$ is zero.*

Proof
Let $r = \alpha p + \beta q$, we can write

$$\begin{aligned} \kappa &= -\underline{B}' \cdot \underline{A} \\ &= -d\underline{P}<r> \cdot df_p<r> \\ &= -II_{f_p}<rr> \\ &= -\alpha^2 II_{f_p}<pp> - 2\alpha\beta\ II_{f_p}<pq> - \beta^2 II_{f_p}<qq> \\ &= -\beta^2 (d\underline{P}<q> \cdot \underline{Q})(\kappa_p - \kappa_q)/\kappa_p. \end{aligned}$$

Now $\beta = 0$ implies we have an A_4 (swallowtail) point, and $\kappa_p = \kappa_q$ implies we are at an umbilic point. Hence away from swallotail points and umbilics κ is zero if and only if $d\underline{P}<q> \cdot \underline{Q}$ is zero. This generically only occurs at isolated points on the cuspidal edge. □

3 Special Points on the Surface

We now examine the special points which lie on the ridges and sub-parabolic lines. There are a number of circumstances which can occur:

1. The ridge is tangent to a line of curvature.
2. The sub-parabolic line is tangent to a line of curvature.
3. The ridge and sub-parabolic line cross.
4. The ridge crosses a ridge of the other colour.
5. The sub-parabolic line crosses a sub-parabolic line of the other colour.
6. Umbilic points.

We shall now examine these situations in more detail.

It is well known that when the red-ridge is tangent to a red-line of curvature (Fig. 5a), we have a swallowtail point on the red-sheet of the focal surface, see [13]. This can be easily seen by noting that when the tangent to the ridge r is in the principal direction p then $df_p<r>$ is zero, so the cuspidal edge must be singular. In fact there are two different types of swallowtail points depending on how the regions of positive and negative Gaussian curvature are arranged. One type of swallowtail is shown in figure 6a.

We have a similar result when the red-sub parabolic line is tangent to a blue-line of curvature (Fig. 5b). Instead of a swallowtail point we have a *cusp of Gauss* (Fig. 6b), whose dual is a swallowtail point. A cusp of Gauss is a point on a parabolic line where the parabolic line is tangent to the principal direction with zero principal curvature. This can also be thought of as a point where a ridge on the focal surface crosses a parabolic line.

Theorem 8 *The following three statements are equivalent:*

1. *The red-sub-parabolic line is tangent to the blue-line of curvature.*
2. *The blue line of curvature has a higher geodesic inflection.*
3. *The red sheet of the focal surface has a cusp of Gauss.*

Proof
First we shall prove that 1 and 2 are equivalent. For a higher geodesic inflection along a line of curvature we require that both the geodesic curvature and its derivative are zero. Now the geodesic curvature of a blue line of curvature is $g = d\underline{P}<q> \cdot \underline{Q}$ and for a higher geodesic inflection we require that $dg<q> = 0$. The equation of the sub-parabolic line is $g = 0$ hence the tangent, r, satisfies $dg<r> = 0$. When the sub-parabolic line is non singular, the case here, this equation is only satisfied for one direction r. We can instantly see that when the sub-parabolic line is in the $\underline{Q}$ direction then we have the condition for a higher inflection. To show the result the other way requires the observation that $d(d\underline{P}<q> \cdot \underline{Q})<p>$ is generically non zero.

Now consider the parabolic line on the red-sheet of the focal surface. When the sub-parabolic line is tangent to a blue-line of curvature then the parabolic line on the focal surface is tangent to $df_p<q>$ which is the principal direction on the focal surface. This is the condition for a cusp of Gauss. □

When a red-sub-parabolic line is tangent to a red line of curvature (Fig. 5c), we observe that the parabolic line on the focal surface is tangent to $\underline{N}$. The

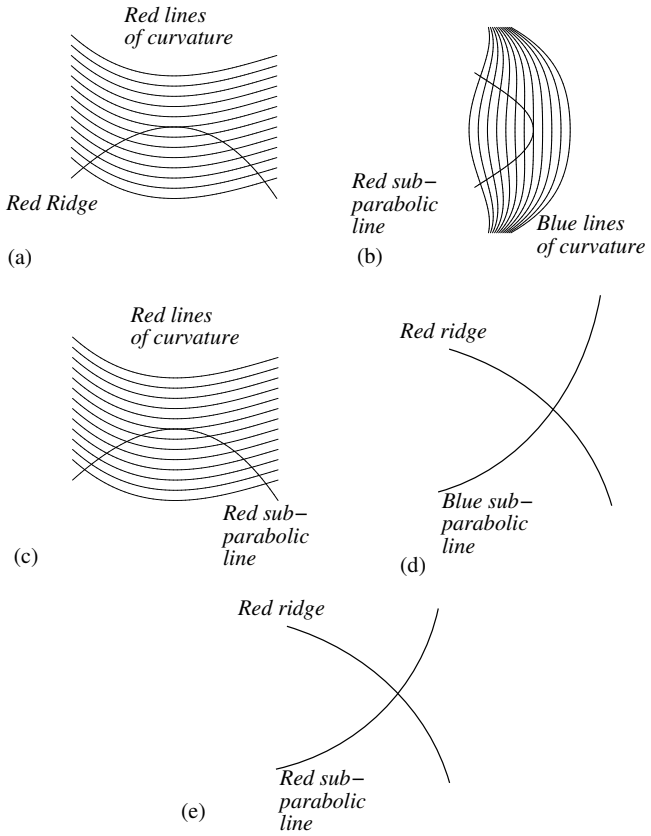

Figure 5: The arrangement of ridges, sub-parabolic lines and lines of curvature at various special points on a surface

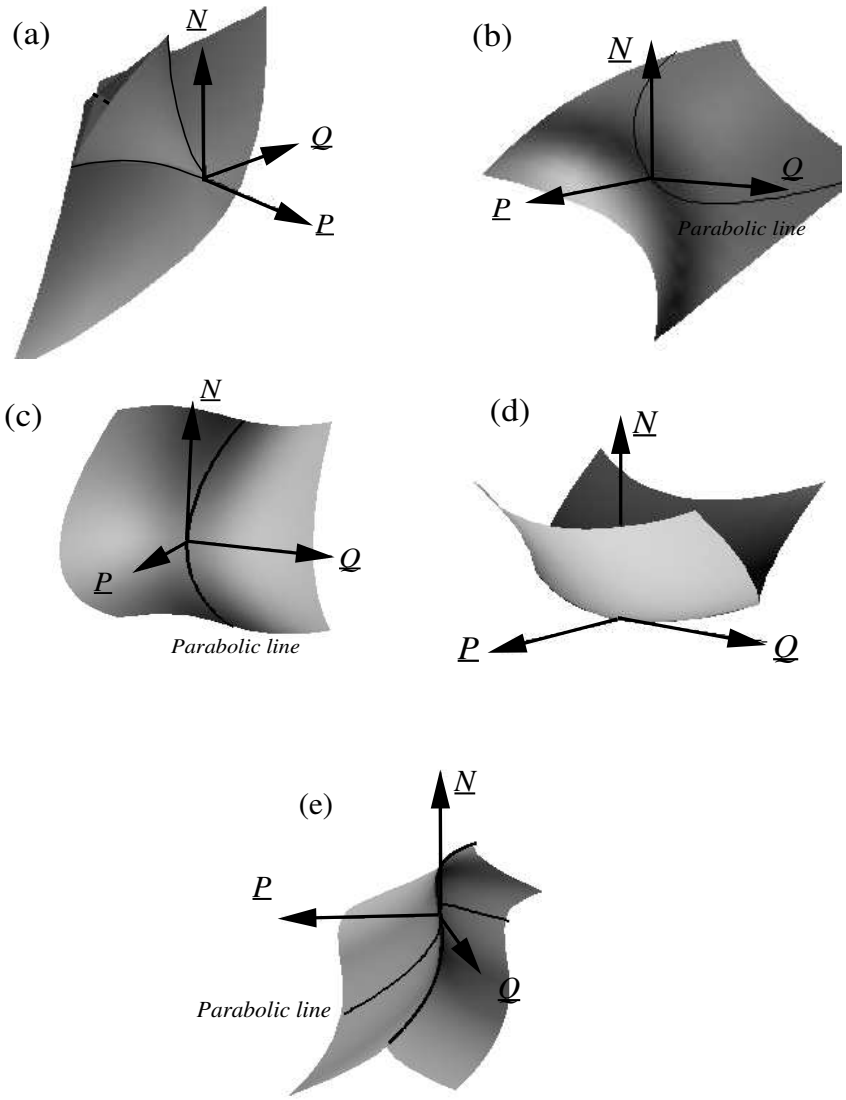

Figure 6: The focal surface for various special points on the surface

parabolic line is tangent to a principal direction, but this does not give a cusp of Gauss as the direction is not the one with zero principal curvature (Fig. 6c).

When a red-ridge crosses a blue sub-parabolic line (Fig. 5d), we observe that $d\kappa_p<r> = 0$ for all tangent vectors r. The cuspidal edge on the red sheet of the focal surface will be tangent to $\underline{Q}$ (Fig. 6d).

When a red-ridge crosses a red-sub-parabolic line (Fig. 5e), we see from Lemma 7 above that a parabolic line will passes through the cuspidal edge and the normal curvature of the edge will change (Fig 6e). The Gaussian curvature of the focal surface is $K = \kappa_p\kappa_q$ so at these points $dK<p> = 0$. At such points the surface will be locally symmetric about the plane containing $\underline{N}$ and $\underline{Q}$. We will get a higher degree of symmetry when the lines are tangent. A special case of this is when the whole surface is symmetrical about a plane. The line of symmetry will be both a ridge and a sub-parabolic line, as well as a line of curvature and a geodesic.

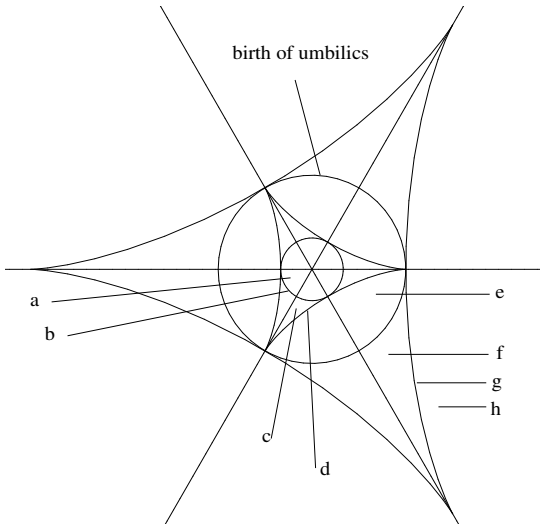

Figure 7: The division of the β-plane according to the type of umbilic.

3.1 Umbilics

Umbilics are points which closely approximate a sphere: every direction through the umbilic is principal and the corresponding curvatures are all equal. A Monge form parametrisation of an umbilic is

$$z = \frac{1}{2\kappa}(x^2 + y^2) + \frac{1}{6}(ax^3 + 3bx^2y + 3cxy^2 + dy^3) + O(4).$$

The type of the umbilic is determined by the cubic terms a, b, c, d. By allowing rotation and scaling of the surface we can represent these cubic terms by a single complex number $\beta = (a + c + i(b + d))/(\omega\bar{\omega}^2)$, where ω is one of the cube roots of $\alpha = (a - 3c + i(d - 3b))$. Actually we need to include a line at infinity, but this will not concern us here. Furthermore, the pattern of ridges, sub-parabolic lines and lines of curvature is determined by where β lies in the diagram shown in figure 7. The corresponding patterns of lines of curvature are shown in figure 8, these are sketched from the computer generated examples first shown in [11]. The patterns of the curves has been theoretically determined in [4, 21, 2, 11].

Inside the smaller circle, the ridges have alternate ordering (red, blue, red, blue, red, blue). On the smaller circle two of the ridges are tangent. Outside the circle but inside the small tri-cusp figure the ordering is red, red, red, blue, blue, blue. As we cross the smaller hypercycloid, we have a cusp transition on the ridges, and the number of ridges drops from three to one. Furthermore, the type of the umbilic changes from being an elliptical umbilic to being a hyperbolic umbilic, the transitionary case is called a parabolic umbilic. Inside this hypercycloid we observe that for the red-sheet of the focal surface, which is an elliptical umbilic, the ordering of cusp edges and parabolic lines is: cusp, cusp, parabolic, cusp, parabolic, parabolic.

Outside the smaller hypercycloid we have an hyperbolic umbilic, with only one ridge running through it. However the pattern of sub-parabolic lines and lines of curvature change. There are three patterns of lines of curvature, the *Star*, *Monstar*, and *Lemon*, these were discovered by Darboux [5], named by Hannay, and their configuration has been proved in [19]. An elegant proof has receintly been demonstrated in [1]. It can be shown, [11][pp144–145], that except at the birth of umbilics, the sub-parabolic lines are tangent to the exceptional lines of

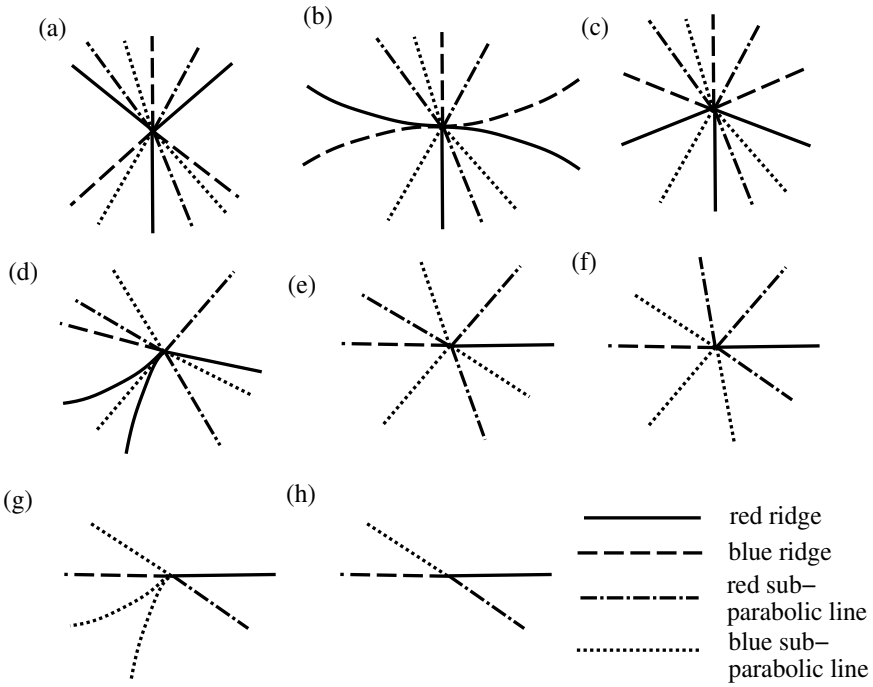

Figure 8: The different patterns of ridges and sub-parabolic lines at umbilics

curvature which pass through the umbilic. Hence we can use information from the sub-parabolic lines to determine the pattern of lines of curvature and vica-versa. Inside the larger circle the sub-parabolic lines have alternate ordering, and the lines of curvature form the star pattern. Between the large circle and the outer hypercycloid, we have a red, red, red, blue, blue, blue ordering, and outside the outer hypercycloid there is only one sub-parabolic line which changes from red to blue.

The three straight lines correspond to symmetrical umbilics, here one of the ridges and one of the sub-parabolic lines are tangent.

The larger circle is special, and corresponds to the birth of umbilics. Umbilics are born and annihilate in pairs, one of which has a star pattern of lines of curvature, the other has a monstar pattern. The moment of the birth corresponds to an umbilic lying on this circle. The pattern of subparabolic lines during such transitions has only reciently been discovered by F.Tari [2] and myself. One such transition is shown in figure 9. There are two other possibilities, either: (a) two ellipses shrink to a point and then disappear, or b) there are five lines through the transitional umbilic which break up into two sets of hyperbola. There are actually three different varieties of this last case determined by the ordering of the colours of the sub-parabolic lines.

4 Implementation

Many of the results and diagrams presented here have been derived from a computer program for calculating ridges, sub-parabolic lines and focal surfaces. This program is described in detail in [11]. The main problems we encounter are finding general formulae for calculating the curves and problems associated with finding orientations for the principal directions.

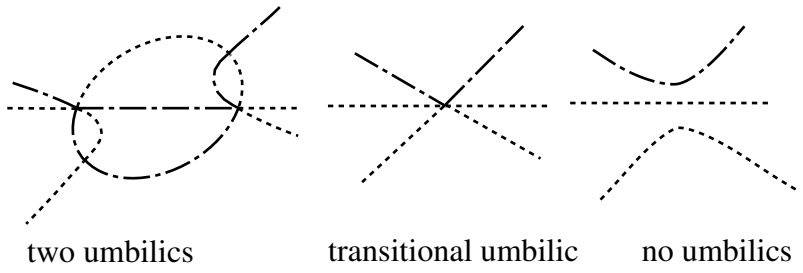

Figure 9: The pattern of sub-parabolic lines for one type of the birth of umbilics transition.

4.1 Practical formulae for calculating ridges and sub-parabolic lines

The above formulae for ridges and sub-parabolic lines are quite difficult to calculate explicitly, as they involve differentiating the principal curvatures. Below we present formulae for these curves for surfaces which are defined either as a parametrised surface by $s : \mathbf{R}^2 \to \mathbf{R}^3$, or by an implicit equation $g(x) = 0$ where $f : \mathbf{R}^3 \to \mathbf{R}$.

For a parametrised surface we use the distance squared map $V : \mathbf{R}^2 \times \mathbf{R}^3 \to \mathbf{R}$ given by

$$V(x, c) = \frac{1}{2}(s(x) - c) \cdot (s(x) - c).$$

This gives half the square of the distance between the point on the surface $s(x)$ and a general point in space c. Let V_1, V_2 and V_3 be the first, second and third order directional derivative of V with respect to x, i.e. we calculate the derivatives keeping c fixed. We have

$$\begin{aligned} V_1<u> &= (s(x) - c) \cdot ds<u>, \\ V_2<uv> &= (s(x) - c) \cdot d^2s<uv> + ds<u> \cdot ds<v>, \\ V_3<uvw> &= (s(x) - c) \cdot d^3s<uvw> + d^s<uv> \cdot ds<w> \\ &\quad + d^2s<uw> \cdot ds<v> + d^2s<vw> \cdot <u>. \end{aligned}$$

We can show, see [11, pp124–130], that

$$\begin{aligned} df_p<p> \cdot \underline{N} &= \frac{1}{\kappa_p} V_3<p^3>, \\ d\underline{P}<q> \cdot \underline{Q} &= 2d^2s<pq> \cdot \underline{Q} - \frac{V_3<pq^2>}{V_2<q^2>}, \end{aligned}$$

where $c = f_p(x)$. In essence these equations are derived by differentiating the equation $V_2<p*> = 0$ with $c = f_p(x)$ in the directions p and q. In practice we use the two formulae

$$\begin{aligned} V_3<p^3> &= 0, \\ 2V_2<q^2>d^2s<pq> \cdot Q - V_3<pq^2> &= 0 \end{aligned}$$

to determine the red ridges and sub-parabolic lines. The principal direction can be calculated by solving the eigen value problem,

$$\begin{pmatrix} l & m \\ m & n \end{pmatrix} \begin{pmatrix} p_1 \\ p_2 \end{pmatrix} = \kappa_p \begin{pmatrix} E & F \\ F & G \end{pmatrix} \begin{pmatrix} p_1 \\ p_2 \end{pmatrix},$$

where $E = I<\underline{ii}>$, $F = I<\underline{ij}>$, $G = I<\underline{jj}>$, $l = II<\underline{ii}>$, $m = II<\underline{ij}>$, $n = II<\underline{jj}>$, and $p = p_1\underline{i} + p_2\underline{j}$. This can be expressed as $II<p*> = \kappa_p I<p*>$ or $V_2<p*> = 0$. One point to note is that the equations for the ridges and sub-parabolic lines depend on the orientation of the principal directions. However the eigen value problem does not give us oriented vectors.

For an implicitly defined surface, $g(x) = 0$, the expressions are much simpler. We have

$$\begin{aligned}
dg<\underline{u}> &= \alpha\underline{N}\cdot\underline{u},\\
dg<\underline{P}> &= 0,\\
d^2g<\underline{uv}> &= d\alpha<\underline{u}>\underline{N}\cdot\underline{v} + \alpha d\underline{N}<\underline{u}>\cdot\underline{v},\\
d^2g<\underline{PP}> &= \alpha d\underline{N}<\underline{P}>\cdot\underline{P} = \kappa_p dg<\underline{N}>,\\
d^2g<\underline{PQ}> &= 0.
\end{aligned}$$

Differentiating the second and fourth of these equations in the direction u gives

$$\begin{aligned}
d^2g<\underline{Pu}> + dg<d\underline{P}<\underline{u}>> &= 0,\\
d^3g<\underline{PPu}> + 2d^2g<\underline{P}d\underline{P}<\underline{u}>> &= d\kappa_p<\underline{u}>dg<\underline{N}> + \kappa_p d^2g<\underline{Nu}>\\
&\quad +\kappa_p d^2g<d\underline{N}<u>>.
\end{aligned}$$

We can eliminate $d\underline{P}<\underline{u}>\cdot\underline{N}$ from these to show

$$\begin{aligned}
dg<\underline{N}>d^3g<\underline{PPu}> - 2d^2g<\underline{PN}>d^2g<\underline{Pu}> &- d^2g<\underline{Nu}>d^2g<\underline{PP}>\\
&= (dg<\underline{N}>)^2 d\kappa_p<\underline{u}>.
\end{aligned}$$

Multiplying by $(dg<\underline{N}>)^2$ and substituting $\underline{u} = \underline{P}$ and $\underline{u} = \underline{Q}$ gives us equations for a red ridge

$$dg<\underline{N}>d^3g<\underline{PPP}> - 3d^2g<\underline{PN}>d^2g<\underline{PP}> = 0,$$

and a blue sub-parabolic line

$$dg<\underline{N}>d^3g<\underline{PPQ}> - d^2g<\underline{QN}>d^2g<\underline{PP}> = 0.$$

Likewise the equation for a blue ridge line is

$$dg<\underline{N}>d^3g<\underline{QQQ}> - 3d^2g<\underline{QN}>d^2g<\underline{QQ}> = 0,$$

and the equation for a red sub-parabolic line is

$$dg<\underline{N}>d^3g<\underline{PQQ}> - d^2g<\underline{PN}>d^2g<\underline{QQ}> = 0.$$

Again we have an eigen-value problem to find the two principal directions. We require $dg<\underline{Q}> = 0$, $d^2g<\underline{PQ}> = 0$ and $\underline{P}\cdot\underline{Q}$. Treating each of these as a map from $\mathbf{R}^3$ to $\mathbf{R}$ we have $M(\underline{P})\underline{Q} = 0$ where $M(\underline{P})$ is the matrix

$$\begin{pmatrix}
dg<\underline{i}> & dg<\underline{j}> & dg<\underline{k}>\\
d^2g<\underline{Pi}> & d^2g<\underline{Pj}> & d^2g<\underline{Pk}>\\
\underline{P}\cdot\underline{i} & \underline{P}\cdot\underline{j} & \underline{P}\cdot\underline{k}
\end{pmatrix}$$

We can solve the equations $det(M(\underline{P})) = 0$, $dg<\underline{P}> = 0$, $\underline{P}\cdot\underline{P} = 1$ to give us our unit length principal directions.

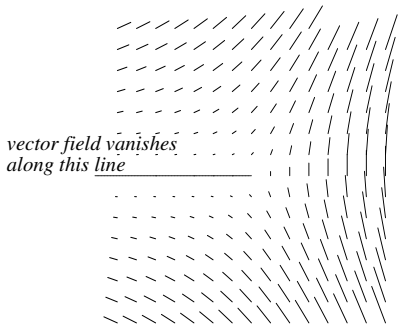

Figure 10: A vanishing oriented principal direction field about an umbilic

4.2 Problems with orientation

The tasks of finding the ridges or sub-parabolic lines on a parametrised surface is essentially the task finding the zero set of $V_3<ppp>$ or $V_3<pqq> - 2d^2 s<pq> \cdot \underline{Q}$, which can be achieved by looking for changes in sign. These equations depend on the orientation of the principal directions. If we take the opposite orientation for the principal direction then $V_3<ppp>$ will change in sign. About an umbilic the index of the principal direction field is $\pm\frac{1}{2}$. Hence it is impossible to find a continuous, non-vanishing *oriented* principal direction vector field. We can however find two vanishing oriented principal direction vector fields from the eigen value problem say $p = (a(x), b(x))$ and $p = (c(x), d(x))$. Each of these equations will give zero length vectors along some line radiating out from the umbilic. The only time both fields vanish at the same point is at umbilics. On either side of the line the principal directions will point in opposite directions (Fig. 10). Moreover, we can see that the ridges cannot be the zero set of any bounded function as there is always an odd number of ridges at each umbilic.

If we want to find a solution to $V_3<ppp> = 0$ along a line segment, we first calculate the principal direction at each point using the first of the expressions. We check that they both point in the same direction by taking the dot product. If the dot product is close to 1, we assume they have the same orientation, and we can test for zeros by seeing if the sign of $V_3<ppp>$ changes. If the dot product is close to -1 then we assume the vector has flipped direction. In such a case we use the other expression for the principal directions, and repeat the process. It is possible for the dot product to be close to zero, which may happen near umbilics. In such a situation we split the line segment into two halves, testing each half for zeros. Once we have a continuous non-vanishing oriented vector field we can test the signs of $V_3<ppp>$ at the end points. If the two signs are different we can use a standard binary sub-division algorithm to converge to the solution.

4.3 Tracing the Curves

To find the complete curve, we use a zero following algorithm. A fairly novel approach bassed on triangles has been used. Given a triangle which has a solution on one side (Fig. 11a) we expect to find one solution on the one of the other two sides (Fig. 11b,c). We can then construct a new triangle and repeat the process. If there is either 1 or 3 solutions round the triangle this indicates the presence of an umbilic. The precise location of the umbilic can be found by minimising the function $\kappa_p - \kappa_q$ which is zero at the umbilic.

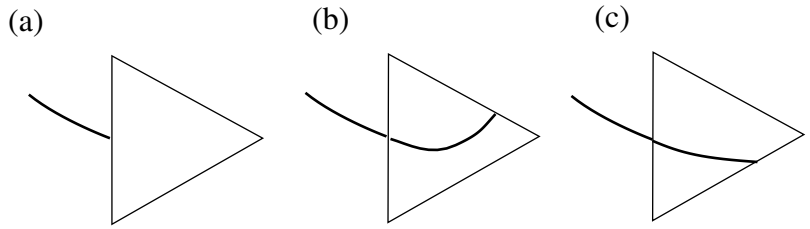

Figure 11: Following a sub-parabolic line

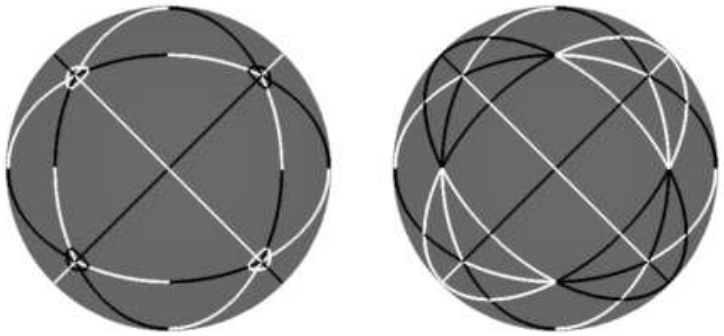

Figure 12: The ridges and sub-parabolic lines for the bumpy cube

Starting points for the curves can be found in two ways. If we take a circle bounding the patch we can step round the circle looking for zeros. We can then use these zeros as starting points. We know that ridges and sub-parabolic lines pass through umbilics. So we can use the umbilics, found earlier in the zero follow routine as starting points. Actually we take a small circle round the umbilic and start from the zeros on that circle. This still leaves the problem of finding closed loops on the ridges such as may be found in the non-generic A_4 transition, (see [13]). Here we can follow the curve $3V_3{<}ppq{>} - V_4{<}pppp{>}V_2{<}qq{>} = 0$ which passes through A_4 points.

Another method for finding the curves is the marching line algorithm which treats the ridges as the intersection of two implicitly defined surfaces [20]. Mike Puddephat [17] has recently been expanding on the work of Markatis [10], in finding the ridges and sub-parabolic lines on bumpy spheres, which are implicitly defined surfaces of the form $f = x^2 + y^2 + z^2 + \epsilon C(x, y, z) - 1 = 0$, where C is a cubic in x, y and z. For small values of ϵ we can closely approximate the bumpy sphere by a unit sphere, and find the points on the sphere which satisfy $d^3f{<}\underline{PPP}{>}df{<}\underline{N}{>} - 3d^2f{<}\underline{PP}{>}d^2f{<}\underline{PN}{>} = 0$. A similar technique as above has been used to calculate the principal directions this time using the implicit formulae. The bumpy spheres provide a rich family of examples for the patterns of ridges and sub-parabolic lines. The pattern of ridges for all the different types of cubics, including the *bumpy cube* (cubic term xyz), the *bumpy orange* ($x^3 - x^2y$), the *bumpy tennis ball* (x^2y), and the *bumpy sphere of revolution* (x^3), are shown in [16]. In the book the colouring of the bumpy cube is incorrect, the correct version, together with the pattern of sub-parabolic lines are shown in figure 12. These pictures have been produced by Mike.

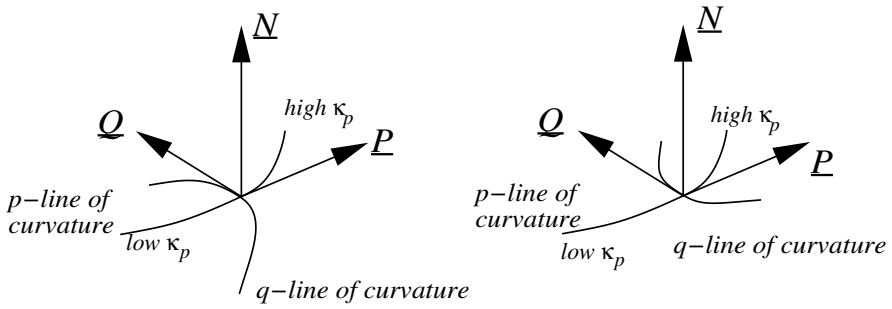

Figure 13: The two types of points on a surface, according to the Gaussian curvature of the focal surface

5 Applications

There are several applications for which the ridges and sub-parabolic lines can be used. One application is to use them for constructing a skeleton of a surface. Rather than using storing all the points on a surface we can just store the points on the curves, greatly reducing the amount of data needed. In [20, 7] such skeletons using only parts of the ridge lines have been used to successfully to compare faces. The problem of reconstructing a surface from such a skeleton has not yet been addressed. The curves may also be used for a measure of "goodness" or "quality" of the surface, the simpler the pattern of ridges and sub-parabolic lines the better. Another method for measuring quality is given in [9].

The formula for the Gaussian curvature of the focal surface gives us a way of segmenting the surface into two parts; we can label points on the surface according to the the sign of the curvature of the focal surface. To see the geometrical meaning of this segmentation we orientate the red principal direction so that it points in the direction of increasing principal curvature, i.e. let p be such that $d\kappa_p<p>>0$. We now have two cases depending on the sign of $d\underline{P}<q> \cdot \underline{Q}$ (Fig. 13). We will switch between the two cases whenever we cross a red ridge or red sub-parabolic line. We cannot produce such a segmentation if we just look for the sign of $V_3<ppp>$ or $d\underline{P}<q> \cdot \underline{Q}$ as both of these equations will change sign if we reverse the principal directions.

One important question is, what does a sub-parabolic line look like? Whilst a satisfactory answer has yet to be found, there are several ways we can spot sub-parabolic points visually. If we look at the surface along some direction $\underline{r}$, then the *apparent contour* of the surface is the set of all points where $\underline{r}$ lies in the tangent plane. The *profile* is the projection of the apparent contour onto a plane normal to $\underline{r}$ (Fig. 14). If $\underline{r}$ is the red principal direction at a point x on the apparent contour then the apparent contour will be tangent to the blue principal direction. Furthermore, the curvature of the profile is equal to the blue principal curvature. If we now consider a motion of the surface so that $\underline{r}$ is always tangent to the line of curvature through x, then we will have a one parameter family of profiles. The curvature of these profiles will change according to $d\kappa_q<p>$. If x lies on a red-subparabolic line then we observe to curvature of the profile has an extremal value at x. The the curvature of the profile will appear to tighten and then relax, as shown in figure 15.

Another way of spotting sub-parabolic points is to examine the geodesic curvature of the apparent contour. If we are looking along a principal direction and x is a sub-parabolic point then the apparent contour will have an inflection at x. For both these methods we need a one parameter family of apparent

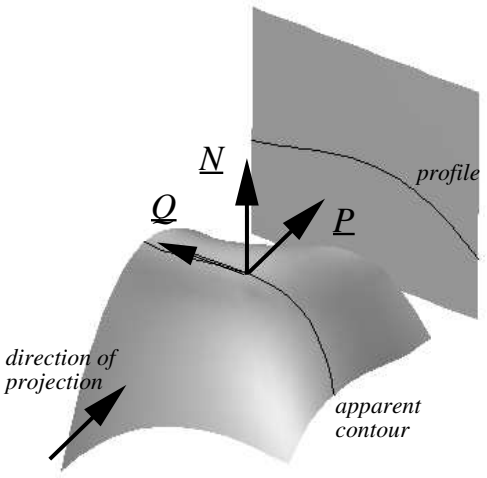

Figure 14: The profile and apparent contour of a surface at a sub-parabolic point

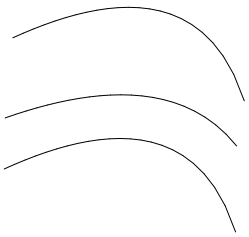

Figure 15: The transition in the profile of a surface as we pass through a point on the sub-parabolic line

contours to determine whether a point lies on a sub-parabolic line. A two parameter family should give the whole line.

References

[1] J.W.Bruce, D.L.Fidal, *On binary differential equations and umbilics*, Proc. Roy. Soc. Edinbrugh, 111A, pp 147-168, 1989.

[2] J.W.Bruce, P.J.Giblin, F.Tari, *Families of Surfaces in Euclidean 3-space, Focal Sets, Ridges and Umbilics*, preprint, University of Liverpool, 1995.

[3] J.W.Bruce, P.J.Giblin, F.Tari, *Ridges, Crests and Sub-Parabolic Lines of Evolving Surfaces*, preprint, University of Liverpool, 1994.

[4] J.W.Bruce, T.C.Wilkinson, *Folding maps and focal sets, Proceedings of Warwick Symposium on Singularities, Springer Lecture Notes in Math.*, vol 1462, pp 63-72, Springer-Verlag, 1989.

[5] G.Darboux, *Leçons sur la théorie générale des surfaces*, 4^{me} Partie, Gauthiers-Villars et Fils, Paris, 1896.

[6] L.P.Eisenhart, *Differential Geometry*, Ginn and Company, Boston, 1909.

[7] C.G.Gordon, *Face recognition from depth maps and surface curvature*, in *Proc. SPIE Conference on Geometric Methods in Computer Vision*, San Diego CA, July 1991.

[8] J.Koenderink, *Solid Shape*, M.I.T. Press, 1990.

[9] G.Liden, A.A.Ball, Intersection Techniques for Assessing Surface Quality, in *Design and Application of Curves and Surfaces. Proc. fifth I.M.A conf. on Mathematics of Surfaces.* III (Edinburgh, 1992), Clarendon press, Oxford, pp. 191–202.

[10] S.Markatis, *Some generic phenomena in families of surfaces in* $\mathbf{R}^3$, Ph.D. Thesis, University of Liverpool, 1980.

[11] R.J.Morris, *Symmetry of Curves and the Geometry of surface: two explorations with the aid of computer graphics,* Ph.D. Thesis, University of Liverpool, 1990.

[12] I.R.Porteous, The normal singularities of a submanifold, *J. Diff. Geom.*, **5**, 543-64, 1971.

[13] I.R.Porteous, The normal singularities of a surface in $\mathbf{R}^3$, *Proc. Sympos. Pure Math.*, Volume 40, Part 2, pp 395–406, American Mathematical Society, 1983.

[14] I.R.Porteous, Ridges and umbilics of surfaces, *The mathematics of surfaces*, II (Cardiff, 1986), Clarendon press, Oxford, pp. 447-58, 1987.

[15] I.R.Porteous, The circles of a surface, *The mathematics of surfaces*, III (Oxford, 1988), Clarendon press, Oxford, pp. 135-43, 1989.

[16] I.R.Porteous, *Geometric Differentiation*, Cambridge University Press, Cambridge, 1994.

[17] M.Puddephat, *Robust fratures of Bumpy Spheres*, M.Sc. Thesis, University of Liverpool, 1994.

[18] J.G.Ramsay, *Folding and fracturing of rocks*, McGraw Hill, New York, 1967.

[19] J.Sottomayer and C.Guttierrez, *Structurally stable configurations of lines of principal curvature,*, Astérisque 98-99, 1982.

[20] J.P.Thirion, A.Gourdon, The Marching Lines Algorithm, new results and proofs, *Rapports de Recherche*, No 1881, INRIA, Sophia Antipolis, France, 1993.

[21] T.Wilkinson, *The geometry of folding maps,* Thesis, University of Newcastle, 1991.